A Scale-constrained Multi-source Photogrammetric Survey for Archaeological Documentation: Methodological Choices, Accuracy Assessment, and Critical Evaluation

Alessio Altadonna [1], Maria Teresa Campisi [2], Andrea Di Santo [3]

[1] Dept. of Engineering, University of Messina, Piazza Salvatore Pugliatti, 1 – 98122 Messina, Italy - alessio.altadonna@unime.it
[2] Dept. of Engineering and Architecture, Kore University of Enna, Piazza dell'Università, 94100 – Enna, Italy - teresa.campisi@unikore.it
[3] PhD Student, Dept. of Engineering and Architecture, Kore University of Enna, Piazza dell'Università, 94100 – Enna, Italy - andrea.disanto@unikorestudent.it

Keywords: Low-cost photogrammetry, Multi-source data integration, Terrestrial and UAV survey, Scale control and accuracy assessment, Point cloud processing and analysis, Archaeological documentation.

Abstract

Low-cost and consumer-grade 3D surveying technologies are increasingly employed in cultural heritage documentation, particularly in archaeological contexts where ideal control conditions and professional instrumentation are often unavailable. In this contribution, we report and critically assess an integrated 3D survey conducted on *Insula IV* within the archaeological site of Tindari (Italy), developed under constrained technical and operational conditions. The survey was based on the combined use of UAV and terrestrial photogrammetry as the primary metric framework, selectively complemented by LiDAR data acquired with the integrated sensor of an iPad Pro 11" to improve geometric completeness in areas affected by occlusions and limited accessibility. A scale-controlled image-based workflow was adopted, where metric reliability was established through internal consistency checks and an extensive set of independent control measurements rather than through a full geodetic reference network. The resulting multi-source 3D model was evaluated in terms of metric consistency and usability for architectural and archaeological analysis. The study demonstrates that, despite non-optimal scale constraint distribution and the exclusive use of low-cost sensors, it is possible to obtain traceable and metrically coherent 3D documentation suitable for detailed planimetric restitution, elevation extraction, and stratigraphic interpretation. Rather than proposing a perspective methodology, the paper provides a transparent and reproducible account of the adopted acquisition, processing, and validation strategy, offering a practical reference for similar heritage survey projects developed under limited resources.

1. Introduction

The growing demand for reliable three-dimensional documentation of cultural heritage has accelerated the adoption of *image-based* and *range-based* surveying approaches – most notably close-range photogrammetry and laser scanning – for analysis, conservation planning, and long-term documentation (Murtiyoso et al., 2021; Musicco et al., 2021; Calisi et al., 2023; Xing et al.; 2025). In parallel, the increasing availability of low-cost sensors and customer-grade platforms has broadened access to 3D surveying, while raising well-known issues concerning metric traceability, uncertainty communication, and repeatability of processing choices (Murtiyoso et al., 2023; Musicco et al., 2023; Kartini et al., 2022).

Archaeological complexes often combine irregular geometry, heterogeneous materials, stratified construction phases, and accessibility constraints. These conditions can prevent "ideal" acquisition configurations and encourage multi-source integration – e.g., aerial and terrestrial photogrammetry complemented by mobile LiDAR – to improve completeness (Teppati Losè et al., 2022; Tian et al., 2025). However, integrating heterogeneous datasets requires an explicit hierarchy of references, well-defined alignment strategies, and clear statement of the metric implications associated with each sensor and acquisition modality, especially when robust geodetic control is unavailable (Kartini et al., 2022; Murtiyoso et al., 2023).

Within this framework, the present contribution does not propose a prescriptive or optimised survey method. Instead, it reports a critically assessed survey experience developed under constrained technical and operational conditions, explicitly documenting decision-making, limitations, and achievable levels of metric reliability. The survey was conducted during an early research/training phase and is here re-examined through an error-aware perspective. The objective is to show how consciously designed methodological choices – despite non-optimal configurations – can still yield usable and traceable 3D documentation, while clearly delimiting the conditions under which results remain interpretable and reusable (Musicco et al., 2023; Murtiyoso et al., 2021).

2. Archaeological and Architectural Context of the Case Study

The case study concerns *Insula IV*, an architectural aggregate within the archaeological area of Tindari (northeastern Sicily), set on a terraced slope overlooking the Tyrrhenian coast. The broader urban context is characterized by an orthogonal street grid structured by *decumani (E-W)* and *cardines/cardi (N-S)*. *Insula IV* belongs to this urban fabric and presents a multi-phase configuration, reflecting long-term occupation and reuse. From a morphological standpoint, the *insula* is defined by a rectangular plan elongated along the N-S direction, bounded longitudinally by two *cardi* and transversely by two *decumani*. The preserved structures exhibit heterogeneous masonry techniques, variable wall thicknesses, and stratified construction episodes; the built fabric is discontinuous, affected by partial collapses, truncations, and surface degradation. These conditions directly affect both

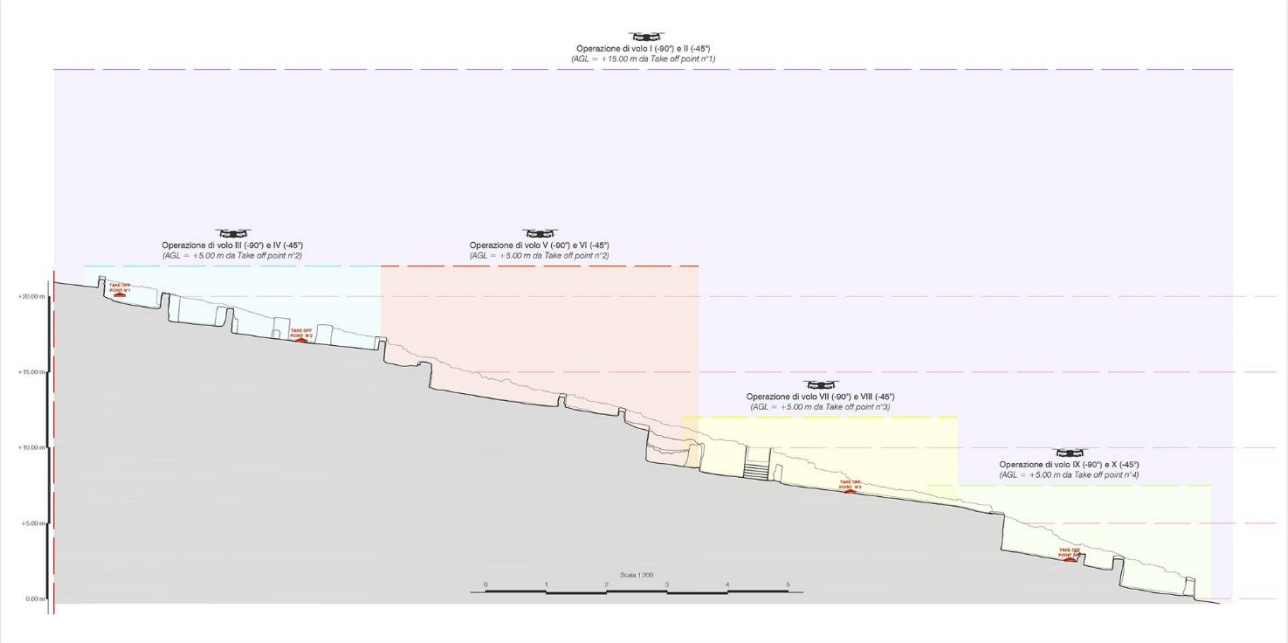

Figure 1. Schematic representation of flight altitudes.

interpretability of architectural evidence and accessibility for data acquisition.

The physical context imposes severe constraints on survey operations. The *cardi* flanking the longitudinal sides of the *insula* are characterised by a pronounced slope – approximately 20 m of elevation difference over 72,50 m of linear development – combined with uneven ground and limited circulation space. This topographic gradient restricts the feasible placement of ground-based controls and complicates linear measurements where slope effects would bias planimetric distances. In addition, several areas are partially inaccessible due to elevation changes, local instability, and protective measures, limiting both terrestrial and UAV line-of-sight continuity.

These morphological and contextual conditions were not treated as generic "difficulties", but as the boundary conditions that determined the survey design. The adopted strategy therefore responds to intrinsic features of the object: articulated geometry, strong height gradient, restricted accessibility, and the limited availability of stable horizontal reference zones. Understanding the architectural and topographical complexity of *Insula IV* is essential for correctly interpreting the choices, limitations and outcomes of the surveying procedures adopted.

3. Survey Design and Methodological Framework

The survey design was formulated by translating explicitly identified boundary conditions into methodological assumptions: (i) absence of a geodetic control network and high-precision topographic instrumentation; (ii) limited feasibility of placing controls with favourable spatial distribution; (iii) strong height gradients along the longitudinal urban axes; and (iv) partial physical accessibility of architectural surfaces. These conditions were assumed as defining parameters for the workflow rather than treated as shortcomings to be "hidden" by generic statements.

Within this context, photogrammetry was adopted as the primary measurement technique because it supports scalable acquisition under heterogeneous constraints and allows the production of dense cloud, 3D mesh and orthomosaics when processing choices are explicitly documented (Murtiyoso et al., 2021; Patrucco et al., 2022). Metric reliability was therefore established through a scale-controlled, image-based approach, supported by internal consistency checks and independent control measurements, rather than by external geodetic referencing. This assumption was declared at design stage and governed processing strategies, validation procedures, and the level of metric confidence attributed to outputs (Musicco et al., 2023).

The strategy was structured hierarchically. UAV photogrammetry provided global geometric coherence and planimetric continuity; terrestrial photogrammetry addressed vertical surfaces, occluded areas, and local detail. Mobile LiDAR data were incorporated selectively to improve completeness in specific zones, without being assigned the role of global metric reference – an approach consistent with reported limitations of consumer mobile LiDAR in range, noise, and stability (Teppati Losè et al., 2022; Klapa et al., 2025; Kartini et al., 2022; Murtiyoso et al., 2023).

Finally, the framework enforced a strict separation between (a) measurement and metric restitution, and (b) interpretative analysis (e.g., stratigraphic reading). 3D models and derived 2D products were treated as measurement-based datasets; interpretative outcomes were developed only after metric processing and consistency assessment were completed. This procedural separation enhances traceability and allows independent critical review of each step, particularly when resource constraints prevent conventional control networks (Teruggi et al., 2021; Bolognesi et al., 2023).

4. Photogrammetric Data Acquisition and Processing

Photogrammetric acquisition was organized into two complementary image blocks – UAV-based and terrestrial – each defined by its intended geometric role within the overall documentation framework (Murtiyoso et al., 2021; Calisi et al., 2023). The UAV block aimed at planimetric continuity and global coherence; terrestrial block targeted vertical surfaces, occlusions, and architectural details insufficiently observable from aerial viewpoints.

4.1. UAV acquisition

UAV imagery was acquired using DJI Mini 3 platform. Flight planning was performed in Dronelink through automated grid

missions, with frontal and lateral overlaps set between 80-85% to provide redundancy for stable camera pose estimation in a context affected by non-uniform terrain and occlusions (Calisi et al., 2023; Tian et al., 2025). Flight altitudes ranged from 5 m to 15 m AGL (Figure 1), selected to maintain a consistent ground sampling distance while respecting safety constraints and obstacle distribution. Both nadir (-90°) and oblique (-45°) camera orientations were acquired: nadir images supported planimetric coherence; oblique images reduced systematic occlusions along walls and stepped structures by improving visibility of vertical and sloped surfaces (Pérez-García et al., 2024; Gómez-López et al., 2025). Image resolution was 12 MP, producing approximately 6.050 aerial images. The dataset supported generation of a site-wide orthomosaic exported at 7,8 mm/px.

4.2. Terrestrial acquisition

Terrestrial photogrammetry documented architectural surfaces and spatial configurations not captured adequately by UAV imagery. Images were acquired using a Sony A5100 mirrorless camera with a 16-50 mm lens. Camera-to-object distances were maintained between ~ 2-5 m, depending on accessibility, safety, and geometry. Acquisition within each sector aimed to maintain consistent geometry (stable distance and viewing angles) and high overlap, supporting robust tie-point extraction across irregular masonry and heterogeneous textures (Patrucco et al., 2022). More than 7.400 terrestrial images were collected, including a dedicated block for high-resolution documentation of selected mosaic pavement.

4.3. Pre-processing and block management

Prior to processing, datasets were segmented by acquisition phase (UAV/terrestrial) and spatial sector. This was done to maintain control over block geometry and reduce alignment instabilities caused by large scale differences and heterogeneous acquisition conditions, as commonly discussed in complex heritage scenes (Musicco et al., 2023; Tian et al., 2025). Uniform basic pre-processing included lens distortion correction and radiometric adjustments to improve feature extraction and reduce artefacts during dense reconstruction and orthomosaic generation (Patrucco et al., 2022).

4.4. SfM processing

Processing was carried out in Agisoft Metashape following a Structure-from-Motion workflow. Alignment used high-accuracy settings with generic preselection, producing a sparse cloud for each block. Bundle adjustment was refined iteratively trough gradual selection steps acting on reprojection error (≤ 1) and reconstruction uncertainty (≤ 100), with repeated camera optimisation after each filtering step. This iterative tie-point cleaning and re-optimisation reflects a documented strategy to improve internal consistency and reduce the influence of poorly constrained points (Mohren et al., 2024). Dense clouds were generated at “Ultra High” quality to preserve geometric detail on irregular masonry and complex surface methodology.

4.5. Orthomosaic

Orthomosaics were computed according to analytical scale. A site-wide orthomosaic derived from the UAV block was exported at 7,8 mm/px, supporting planimetric restitution at architectural scale. A high detail orthomosaic for a selected mosaic pavement was generated from close-range terrestrial imagery, achieving 0,5 mm/px, enabling inspection of tesserae patterns (Figure 2), lacunae, and surface alteration at conservation-oriented detail (Musicco et al., 2023; Rabosh et al., 2022). These raster products were treated as measurement-based representations and used as controlled inputs for subsequent metric restitution workflows.

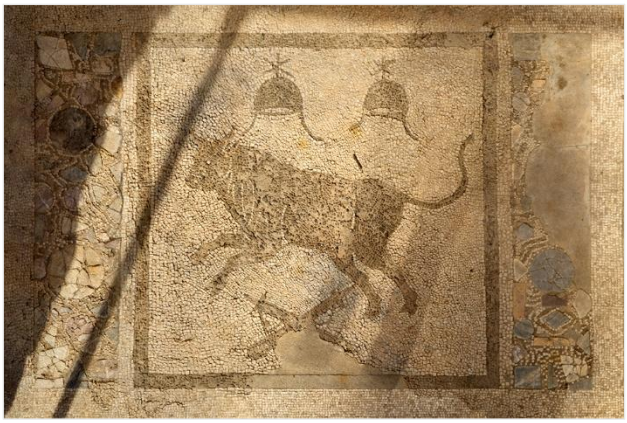

Figure 2. Orthomosaic of the floor mosaic belonging to *apodyterium* no. 2, *Termae*, *Insula IV*.

5. Scale Control and Metric Constraints

Scale definition was critical due to the absence of a geodetic control network and the limited feasibility of distributing ground controls. Under these conditions, scale control was implemented through a reduced number of direct metric constraints, explicitly treated as *scale references* rather than full 3D geometric controls (Musicco et al., 2023; Murtiyoso et al., 2021).

Two scale bars were introduced within the photogrammetric workflow. Both were horizontal and referred to linear distances measured on the ground along the upper *decumanus*, where stable and accessible conditions allowed reliable measurements using a measuring tape and a handled laser distance meter. The constraints were introduced during bundle adjustment in Agisoft Metashape to define the global metric scale of the photogrammetric model.

This configuration was explicitly recognised as non-optimal in both number and spatial distribution. Reducing the number of scale constraints limits redundancy and the capability to detect local inconsistency through multiple independent constraints. However, alternative placements were not feasible due to the physical characteristics of the site: the cardi flanking the longitudinal sides of the insula exhibit steep slope (20 m over 72,50 m). Under such conditions, placing scale constraints along these axes would have required careful reduction of slope distances to horizontal components; without adequate instrumentation and stable reference geometry, such operations would risk introducing systematic bias if distances were treated ad planimetric by simplification. Consequently, scale constraints were deliberately concentrated where measurements could be performed with acceptable reliability and traceability.

Importantly, the adopted configuration is not used here to justify unsupported claims of deformation or anisotropy. Instead, it is stated as a boundary condition that defined the interpretative limits of metric outputs. The workflow therefore prioritised transparency and post hoc verification over artificially increasing constraints in a way that could reduce traceability. This approach aligns with the emphasis – common in low-cost or constrained surveys – on making explicit the relationship between achievable metric confidence and the practical feasibility of control distribution (Murtiyoso et al., 2023; Musicco et al., 2023).

6. Multi-source data Integration (Photogrammetry-LiDAR)

The integration between photogrammetric and LiDAR datasets was conceived as a targheted operation aimed at improving geometric completeness, without altering the metric reference framework established by the photogrammetric model. Since photogrammetry represented the only scale-controlled dataset of the survey, LiDAR information was incorporated selectively in those portions of the site where UAV and terrestrial image acquisition alone did not provide sufficient spatial coverage or visibility (Teppati Losè et al., 2022; Kartini et al., 2022).

LiDAR data were acquired using the integrated LiDAR sensor of an iPad Pro 11", which enables rapid and flexible spatial sampling. However, this type of sensor is characterized by limited range, variable point density, and lower metric stability when compared to dedicated terrestrial laser scanners. For this reason, it was used strictly as complementary geometric support rather than as a primary measurement reference (Teppati Losè et al., 2022; Murtiyoso et al., 2023).

Data integration was performed in CloudCompare, following a hierarchical alignment strategy in which the photogrammetric point cloud constituted the reference geometry. The LiDAR point cloud was subdivided into three independent subsets corresponding to distinct acquisition sessions and spatial sectors. This segmentation ensured full control over local geometry prevented cumulative misalignments across heterogeneous datasets (Kartini et al., 2022).

Alignment was carried out through a rigid point-to-point registration based on manually selected homologous points (minimum $N \geq 3$ per subset), distributed on clearly identifiable and stable geometric features observable in both datasets. In this work, correspondences were established on planar surfaces, edges, and regular architectural elements, minimizing interpretative ambiguity caused by differences in density and noise between photogrammetric and iPad LiDAR data (Kartini et al., 2022; Fazion et al., 2024).

No Iterative Closest Point (ICP) refinement was applied. This decision was deliberate, as automated cloud-to-cloud minimisation procedures may introduce artificial deformations when datasets originate from sensors with significantly different sampling characteristics. Maintaining a strictly manual, rigid registration preserved the metric hierarchy defined by the photogrammetric workflow and ensured full traceability of alignment decisions (Teppati Losè et al., 2022; Bassier et al., 2024; Murtiyoso et al., 2023).

After alignment, the LiDAR subsets were merged with the photogrammetric cloud to enhance local geometric completeness. The resulting dataset was treated as a composite representation in which the origin, density, and metric reliability of each source remained explicitly distinguishable. This approach ensured that multi-source integration improved interpretative usability while maintaining transparency regarding data provenance and geometric consistency (Fazion et al., 2024; Yang et al., 2023).

7. Accuracy Assessment and Consistency Analysis

Metric quality was assessed through a structured multi-level framework designed to produce verifiable evidence. Rather than estimating absolute accuracy – methodologically unjustified under the boundary conditions – the analysis focused on internal consistency, scale reliability, and relative agreement between independent measurements and model-derived quantities (Musicco et al., 2023; Murtiyoso et al., 2021).

Beyond the two scale bars used for global scale definition during bundle adjustment, approximately 200 independent control measurements were collected on site using a metric tape and a handheld laser distance meter. Measurements were diversified to sample different spatial extents and geometric conditions: (i) perimeters of rooms and enclosed spaces, (ii) diagonals of rooms, (iii) wall thicknesses, and (iv) linear distances between clearly identifiable architectural elements. Each measurement was selected to be directly traceable in the photogrammetric model to minimise ambiguity in point identification, consistent with the need for auditable checks in constrained workflows (Musicco et al., 2023).

For each control segment i, a residual was computed as:

$$\triangle_i = d_i^{model} - d_i^{field}$$

allowing systematic comparison between field observations and model-derived distances. Residual ranged approximately between 1 and 5 cm, with dependence on measurement type and configuration. Short distances (e.g., wall thicknesses, local spans) tended towards the lower bound; larger discrepancies occurred on longer measurements, particularly diagonals spanning rooms with irregular boundaries. This behaviour is consistent with cumulative uncertainty propagation over increasing distance and with the intrinsic limitations of manual measurements in irregular archaeological context, where endpoints may not be perfectly sharp or stable (Murtiyoso et al., 2021; Musicco et al., 2023).

The absence of systematic directional patterns in residuals was treated cautiously: it supports an interpretation of scale stability at the centimetric level but does not prove lack of deformation across all areas. Accordingly, the model is treated as metrically reliable within the declared scale-control configuration and the empirically observed residual envelope, without extrapolating beyond what the independent checks can justify.

Relative consistency checks were also performed against the integrated mobile LiDAR subsets. After rigid point-to-point registration, local agreement and surface-to-surface deviations were inspected in CloudCompare in overlap areas. The intent was not to validate one dataset against the other, but to check their mutual consistency within the instrumental and methodological limits adopted, in accordance with similar evaluation studies on LiDAR integrated on iPad Pro 11" (Kartini et al., 2022; Teppati Losè et al., 2022). Observed local agreement was compatible with the centimetric residual range derived from field controls.

Taken together, the two scale constraints, the extensive independent control measurement set, and the relative coherence checks provide an auditable basis for evaluating metric reliability. The resulting 3D model is not claimed to be absolutely accurate in a geodetic sense; however, it demonstrates internal coherence and scale stability compatible with architectural-archaeological analyses at centimetric level, if interpretations remain bounded by documented uncertainty envelope (Musicco et al., 2023).

8. Metric Outputs and Planimetric Restitution

The photogrammetric survey served as the metric foundation for producing traditional 2D archaeological outputs. Planimetric restitution also acted as a verification stage, since it requires transforming 3D measurement datasets into analytically usable 2D documents under explicit scale and tolerance assumptions (Murtiyoso et al., 2021; Rabosh et al., 2022).

The primary planimetric base was derived from UAV orthomosaic generated exclusively from nadir imagery, minimising angular effects and reducing occlusion-driven geometric artefacts in planimetric reading (Calisi et al., 2023; Pérez-García et al., 2024). The orthomosaic achieved a mean pixel size of 7,8 mm/px (Figure 3) across the insula extent and was adopted as reference resolution. The raster was exported in georeferenced format and imported into CAD environment as a metric underlay for vector restitution.

Figure 3. Orthomosaic of *Insula IV*.

Figure 4. 2D product, detailed floor plan of *Insula IV*.

Vector drawing was executed by tracing wall alignments, room boundaries, circulation paths, and open spaces directly from the orthomosaic, avoiding interpretative regularisation at this stage. Attention was paid to junction continuity, discontinuities and breaks, and the representation of ambiguous areas affected by erosion or occlusion. Where readings were uncertain, uncertainty was preserved as such rather than resolved by graphic assumptions.

A second metric output concerned mosaic pavements. Close-range terrestrial photogrammetry supported orthomosaics at 0,5 mm/px, enabling detailed representation of tesserae arrangement, decorative patterns, lacunae, and alteration traces relevant for descriptive and conservation-oriented tasks (Musicco et al., 2023). This value is explicitly interpreted as raster spatial resolution, not as a proxy for sub-millimetric absolute accuracy; metric confidence remains bounded by the centimetric residuals documented in Section 7.

8.1. Representation scale

Graphic scales were derived from raster resolution and from the observed residual envelope. For the 7,8 mm/px UAV orthomosaic, vector restitution was conducted at scales compatible with the information content (e.g., 1:50-1:100), ensuring that minimum mappable features, line weights, and symbolisation did not imply precision unsupported by the dataset. Graphic tolerances were defined by combining pixel size (as a lower bound of representable detail) with the independent measurement residual range (as a bound on metric reliability). This prevents implicit attribution of precision beyond centimetric reliability and enforces coherence between source data, drawing

scale, and analytical use (Murtiyoso et al., 2021; Musicco et al., 2023).
Overall, the planimetric products (Figure 4) demonstrate that – under controlled and explicitly documented constraints – photogrammetric datasets can support metric 2D documentation traditionally derived from manual survey, if scale, tolerance, and uncertainty statements remain explicitly tried to verifiable checks.

9. 3D-Based Analysis and Stratigraphic Interpretation

The 3D photogrammetric dataset was used as a metric analytical framework for investigating architectural elevations and masonry stratigraphy. Dense clouds and mesh products were treated as intermediate geometric datasets enabling controlled extraction of analytical 2D representation, consistent with research emphasising the role of point clouds and derived imagery ad knowledge bases for subsequent semantic/interpretative tasks (Teruggi et al., 2021; Bolognesi et al., 2023).

9.1. Section extraction

Sectioning operation was carried out directly on 3D mesh using cutting planes oriented longitudinally and transversely with respect to the insula layout, coherently with the urban axes (*cardines/decumani*). Each plane's position and orientation were defined in strict coherence with the planimetric reference derived from the orthomosaic, ensuring geometric consistency across representations. Section thickness was kept limited to reduce projection ambiguity; for each section, plane parameters (orientation, position, thickness) were documented to guarantee repeatability and traceability.

9.2. Elevation restitution

Extracted sectional profiles were exported and imported into a CAD environment for elevation restitution. Vectorisation traced measured geometry directly, avoiding idealisation unless supported by the data. Cross-checks between planimetric outlines, section traces, and elevations were performed to prevent inconsistencies introduced by independent reinterpretation of different views.

9.3. Orthomosaics and stratigraphic mapping

Orthomosaics of vertical surfaces were generated and imported into CAD as raster underlays to support stratigraphic analysis. Raster products preserved both metric coherence and radiometric information, enabling observation of bonding patterns, material variation, texture change, and discontinuities (Figure 5). Stratigraphic units were delineated using dedicated layers and hatching conventions. Importantly, stratigraphic interpretation was executed as a distinct analytical phase after metric restitution, maintaining a clear procedural separation between measured geometry and interpretative classification – an approach consistent with broader research on semantic enrichment and stratigraphy-oriented digital workflows (Teruggi et al., 2021; Garozzo et al., 2024; Nespeca et al., 2024; Lombardi et al., 2025).
This chain – from measured 3D geometry to sections/elevations, to orthomosaic-supported stratigraphic mapping – preserves traceability. The 3D dataset functions as an analytical environment that supports stratigraphic reasoning while constraining interpretation to auditable metric evidence, aligning with the emphasis on transparent, reproducible knowledge extraction from survey data (Yang et al., 2023; Buldo et al., 2024).

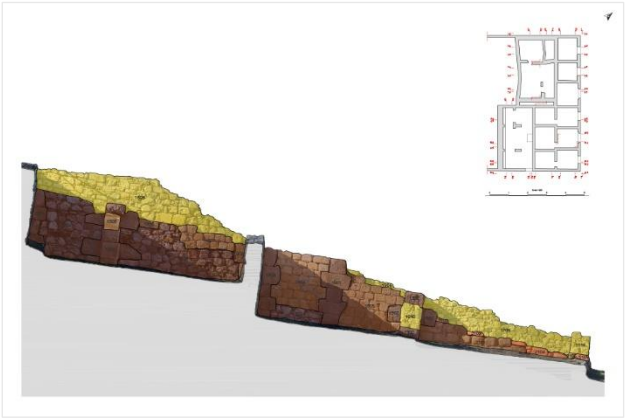

Figure 5. Stratigraphic analysis of the elevations, Section 9-9.

10. Discussion and Critical Evaluation

The survey experience must be interpreted in relation to explicit boundary conditions: absence of a geodetic network, limited scale constraints, and severe morphological/accessibility constraints. Under these conditions, results are not discussed in terms of absolute accuracy alone, but through internal consistency, transparent uncertainty disclosure, and fitness-for-purpose for intended analytical tasks (Murtiyoso et al., 2021; Musicco et al., 2023).
Adopting photogrammetry as primary scale-controlled reference, complemented by selective mobile LiDAR integration, proved coherent with the site's physical characteristics and resource constraints. The hierarchical organization of data sources, explicit declaration of metric assumptions, and separation between measurement and interpretation maintained control over geometric reliability. Rather than compensating for missing instrumentation through implicit claims, the workflow prioritised traceability and documented verification strategies, reflecting good practice in constrained low-cost contexts (Murtiyoso et al., 2023; Kartini et al., 2022).
Consistency assessment indicated centimetric-level residuals over a wide set of independent checks, supporting the use of the dataset for architectural-archaeological analyses at that scale. At the same time, the limited distribution of scale constraints is explicitly acknowledged as a factor that bounds interpretability: it does not invalidate the survey, but defines the responsible operational limits for metric reuse. In this sense the contribution in less about proposing "a method" than about demonstrating how methodological transparency, auditable checks, and explicit limitation statements can produce scientifically usable outcomes when ideal conditions are unattainable (Musicco et al. 2023; Murtiyoso et al., 2021).

11. Conclusion and Future Development

This contribution presented a critically assessed survey experience conducted under constrained technical, logistical, and economic conditions. The work documents a coherent and transparent workflow in which survey design, acquisition, processing, and analysis were derived from the physical and operational characteristics of the archaeological context.
The integration of UAV and terrestrial photogrammetry supported by selective use of mobile LiDAR, produced metrically consistent datasets suitable for architectural and archaeological analysis at centimetric scale. Despite the limited number and unilateral distribution of scale constraints, independent control measurements and relative consistency checks provide auditable evidence that the resulting model is

reliable within clearly defined limits (Musicco et al., 2023; Teppati Losè et al.; 2022).
Derived products – planimetric restitutions, high-resolution orthomosaics, sectional profiles, and stratigraphic mappings – demonstrate the analytical potential of 3D survey datasets when treated as structured measurement environments rather than as purely visual deliverables. The workflow highlights the importance of separating metric restitution from interpretative analysis to preserve traceability and reproducibility (Teruggi et al., 2021; Nespeca et al., 2024).
Future developments will focus on refining scale control strategies (increasing redundancy and improving spatial distribution where feasible), integrating additional independent measurements, and extending the approach to comparative case studies. The experience documented here supports informed decision-making through methodological transparency rather than instrument-driven claims of precision (Murtiyoso et al., 2023; Xing et al., 2025).

References

Bassier, M., Mazzacca, G., Battisti, R., Malek, S., and Remondino, F. (2024). Combining Image and Point Cloud Segmentation to Improve Heritage Understanding, *Int. Arch. Photogramm. Remote Sens. Spatial Inf. Sci.*, XLVIII-2/W4-2024, 49–56, https://doi.org/10.5194/isprs-archives-XLVIII-2-W4-2024-49-2024

Bolognesi, C. M. and Bassorizzi, D. (2023) Scan to BIM Processes: Heritage Accuracy Versus BIM Semantic, *Int. Arch. Photogramm. Remote Sens. Spatial Inf. Sci.*, XLVIII-M-2-2023, 267–272, https://doi.org/10.5194/isprs-archives-XLVIII-M-2-2023-267-2023

Buldo, M., Agustín-Hernández, L., & Verdoscia, C. (2024). Semantic Enrichment of Architectural Heritage Point Clouds Using Artificial Intelligence: The Palacio de Sástago in Zaragoza, Spain. *Heritage*, *7*(12), 6938-6965. https://doi.org/10.3390/heritage7120321

Calisi, D., Botta, S., and Cannata, A. (2023). Integrated Surveying, from Laser Scanning to UAV Systems, for Detailed Documentation of Architectural and Archeological Heritage. *Drones*, *7*(9), 568. https://doi.org/10.3390/drones7090568

Fazion, B., Treccani, D., Fregonese, L., and Lombardini, N. (2024). HBIM Structural Model to Evaluate Building Evolution and Construction Hypotheses: Preliminary Results, *Int. Arch. Photogramm. Remote Sens. Spatial Inf. Sci.*, XLVIII-2/W4-2024, 213–219, https://doi.org/10.5194/isprs-archives-XLVIII-2-W4-2024-213-2024

Garozzo, R., Riveiro Rodríguez, B., and Santagati, C. (2024). 3D Segmentation and Analysis for Masonry Bridge Preservation, Int. Arch. Photogramm. *Remote Sens. Spatial Inf. Sci.*, XLVIII-4/W11-2024, 17–23, https://doi.org/10.5194/isprs-archives-XLVIII-4-W11-2024-17-2024

Gómez-López, J. M., Pérez-García, J. L., Mozas-Calvache, A. T., and Vico-García, D. (2025). Analysis of the Photogrammetry Use of Videos from 360-Degree Multicameras in Heritage-Related Scenes: Case of the Necropolis of Qubbet El-Hawa (Aswan, Egypt), *Int. Arch. Photogramm. Remote Sens. Spatial Inf. Sci.*, XLVIII-M-9-2025, 533–539, https://doi.org/10.5194/isprs-archives-XLVIII-M-9-2025-533-2025

Kartini, G. A. J., Gumilar, I., Abidin, H. Z., and Yondri, L. (2022). The Comparison of Different LiDAR Acquisition Software on iPad Pro M1, *Int. Arch. Photogramm. Remote Sens. Spatial Inf. Sci.*, XLVIII-2/W1-2022, 117–120, https://doi.org/10.5194/isprs-archives-XLVIII-2-W1-2022-117-2022

Klapa, P., Żygadło, A., & Pepe, M. (2025). 3D Heritage Reconstruction Through HBIM and Multi-Source Data Fusion: Geometric Change Analysis Across Decades. *Applied Sciences*, *15*(16), 8929. https://doi.org/10.3390/app15168929

Lombardi, M., & Dubbini, R. (2025). From Earth to Interface: Towards a 3D Semantic Virtual Stratigraphy of the Funerary Ara of *Ofilius Ianuarius* from the Via Appia Antica 39 Burial Complex. *Heritage*, *8*(8), 305. https://doi.org/10.3390/heritage8080305

Mohren, J., & Schulze, M. (2024). Automated cleaning of tie point clouds following USGS guidelines in Agisoft Metashape professional (ver. 2.1.0). *MethodsX*, *12*, 102679. https://doi.org/10.1016/j.mex.2024.102679

Murtiyoso, A. & Grussenmeyer, P. (2023). Initial Assessment on the Use of State-of-the-art Nerf Neural Network 3D Reconstruction for Heritage Documentation, *Int. Arch. Photogramm. Remote Sens. Spatial Inf. Sci.*, XLVIII-M-2-2023, 1113–1118, https://doi.org/10.5194/isprs-archives-XLVIII-M-2-2023-1113-2023

Murtiyoso, A. & Grussenmeyer, P. (2021). Experiments Using Smartphone-Based Videogrammetry for Low-cost Cultural Heritage Documentation, *Int. Arch. Photogramm. Remote Sens. Spatial Inf. Sci.*, XLVI-M-1-2021, 487–491, https://doi.org/10.5194/isprs-archives-XLVI-M-1-2021-487-2021

Musicco, A., Rossi, N., and Verdoscia, C. (2023). Accuracy Evaluation of Smartphone-based Videogrammetry for Cultural Heritage Documentation Process, *Int. Arch. Photogramm. Remote Sens. Spatial Inf. Sci.*, XLVIII-M-2-2023, 1119–1126, https://doi.org/10.5194/isprs-archives-XLVIII-M-2-2023-1119-2023

Musicco, A., Galantucci, R. A., Bruno, S., Verdoscia, C., and Fatiguso, F. (2021). Automatic Point Cloud Segmentation for the Detection of Alterations on Historical Buildings Through an Unsupervised and Clustering-based Machine Learning Approach, *ISPRS Ann. Photogramm. Remote Sens. Spatial Inf. Sci.*, V-2-2021, 129–136, https://doi.org/10.5194/isprs-annals-V-2-2021-129-2021

Nespeca, R., Mariotti, C., Petetta, L., and Mandriota, A. (2024). Point Cloud Segmentation in Heritage Preservation. Advanced Digital Process for Historical Houses, *Int. Arch. Photogramm. Remote Sens. Spatial Inf. Sci.*, XLVIII-2/W4-2024, 325–332, https://doi.org/10.5194/isprs-archives-XLVIII-2-W4-2024-325-2024

Patrucco, G., Giulio Tonolo, F., Sammartano, G., and Spanò, A. (2022). SfM-Based 3D Reconstruction of Heritage Asset Using UAV Thermal Images, *Int. Arch. Photogramm. Remote Sens. Spatial Inf. Sci.*, XLIII-B1-2022, 399–406, https://doi.org/10.5194/isprs-archives-XLIII-B1-2022-399-2022

Pérez-García, J. L., Gómez-López, J. M., Mozas-Calvache, A. T., & Delgado-García, J. (2024). Analysis of the Photogrammetric Use of 360-Degree Cameras in Complex Heritage-Related

Scenes: Case of the Necropolis of Qubbet el-Hawa (Aswan Egypt). *Sensors*, *24*(7), 2268. https://doi.org/10.3390/s24072268

Rabosh, E. V., Balbekin, N. S., Mezhenin, A. V., and Petrov, N. V. (2022). Application of Photogrammetry for Digitizing Information About Cultural Heritage in the Form of Display Holograms, *Int. Arch. Photogramm. Remote Sens. Spatial Inf. Sci.,* XLIII-B2-2022, 869–875, https://doi.org/10.5194/isprs-archives-XLIII-B2-2022-869-2022

Teppati Losè, L., Spreafico, A., Chiabrando, F., & Giulio Tonolo, F. (2022). Apple LiDAR Sensor for 3D Surveying: Tests and Results in the Cultural Heritage Domain. *Remote Sensing*, *14*(17), 4157. https://doi.org/10.3390/rs14174157

Tian, M., Zheng, C., and Lou, N. (2025). Research on the Integrated Application of Multi-scale 3D Digital Technologies in Village Heritage Conservation, *Int. Arch. Photogramm. Remote Sens. Spatial Inf. Sci.*, XLVIII-M-9-2025, 1499–1506, https://doi.org/10.5194/isprs-archives-XLVIII-M-9-2025-1499-2025

Teruggi, S., Grilli, E., Fassi, F., and Remondino, F. (2021). 3D Surveying, Semantic Enrichment and Virtual Access of Large Cultural Heritage, *ISPRS Ann. Photogramm. Remote Sens. Spatial Inf. Sci.*, VIII-M-1-2021, 155–162, https://doi.org/10.5194/isprs-annals-VIII-M-1-2021-155-2021

Xing, Y., Yang, S., Fahy, C., Harwood, T., & Shell, J. (2025). Capturing the Past, Shaping the Future: A Scoping Review of Photogrammetry in Cultural Building Heritage. *Electronics*, *14*(18), 3666. https://doi.org/10.3390/electronics14183666

Yang, S., Hou, M., & Li, S. (2023). Three-Dimensional Point Cloud Semantic Segmentation for Cultural Heritage: A Comprehensive Review. *Remote Sensing*, *15*(3), 548. https://doi.org/10.3390/rs15030548